Program Digest, 2019 IEEE International Ultrasonics Symposium (IUS)
Glasgow, Scotland, October 6-9, 2019

Theoretical Study of Thermally Stable Large-Coupling SH_0 Plate Wave Resonators

J. Zou*, V. Yantchev, S. Samadian, and P. J. Turner
Resonant Inc.,
Santa Barbara, CA, USA
*E-mail: jzou@resonant.com

V. Plessky
GVR Trade SA and Resonant Inc.,
Gorgier, Switzerland

***Abstract*—The thermal stabilization techniques for the fundamental (SH_0) Plate acoustic wave (PAW) resonators based on $LiNbO_3$ are theoretically investigated in this paper. The SH_0 mode offers an ultra-large coupling coefficient (k^2) at a certain crystal cut angle and normalized plate thickness, but its poor temperature coefficient of frequency (*TCF*) hinders its application in RF systems and needs further improvement urgently. By adding SiO_2 with positive *TCF* to the $LiNbO_3$ plate, a robust temperature compensation approach can be achieved for the SH_0 resonators on $LiNbO_3/SiO_2$ bilayer and $SiO_2/LiNbO_3/SiO_2$ sandwiched structures. The propagation characteristics of the SH_0 wave propagating in the layered medium are carefully investigated. Despite the trade-off between *TCF* and k^2, the $SiO_2/LiNbO_3/SiO_2$ structure provides large k^2 and near-zero *TCF* for wider thickness combinations. Furthermore, the periodic structure dispersion of the simplest zero-*TCF* stack is provided and the critical threshold IDT thickness is given.**

Keywords—Lithium niobate, piezoelectricity, resonators, temperature coefficient of frequency (TCF), thermal stability.

I. Introduction

In response to the drastically increasing demands for ubiquitous wireless connectivity, faster data delivery in wireless mobile, Internet-of-Things (IoT), autonomous vehicles, and artificial intelligence, new services currently go into operation requiring progressively wider frequency bands. The coupling coefficient (k^2) of the commercially popular surface acoustic wave (SAW) or bulk acoustic wave (BAW) technology is between 6%-13%, limiting the filter bandwidth (*BW*) to up to 6%. Both the current bands wider than 6% with tight specifications and the ultra-wide band (> 15%) required by the next-generation re-configurable filters and cognitive radios point the urgent need of micro-acoustic resonators with ultra-large k^2 [1]-[3].

A $LiNbO_3$ plate based SH_0 Plate Acoustic Wave (PAW) resonator characterizes the largest k^2 among all acoustic wave devices, up to 50% in certain cut angles and $LiNbO_3$ thickness [1]. As a result, the SH_0 PAW technology can be an excellent solution to the ultra-wide bands, as well as recently proposed XBARs [4]. However, $LiNbO_3$ features a material property of drastically softening when temperature rises, leading to very poor temperature coefficient of frequency (*TCF*) of ~ -70 ppm/˚C. This poor *TCF* would be unacceptable for any application in current or future RF systems. So an improvement of the thermal stability of $LiNbO_3$-based SH_0 resonators is highly desirable for enabling low-temperature-drift and ultra-wide-band filters [5].

The thermal stability can be achieved by adding SiO_2, which has a positive *TCF* of ~ +80 ppm/˚C to the $LiNbO_3$ plate, forming a robust passive compensation. The SH_0 wave propagation characteristics are carefully investigated after introducing the non-piezoelectric SiO_2 herein and optimized stack proposed for achieving the thermal insensitivity and large k^2 simultaneously. Moreover, the periodic structure dispersion of the simplest zero-*TCF* stack is provided.

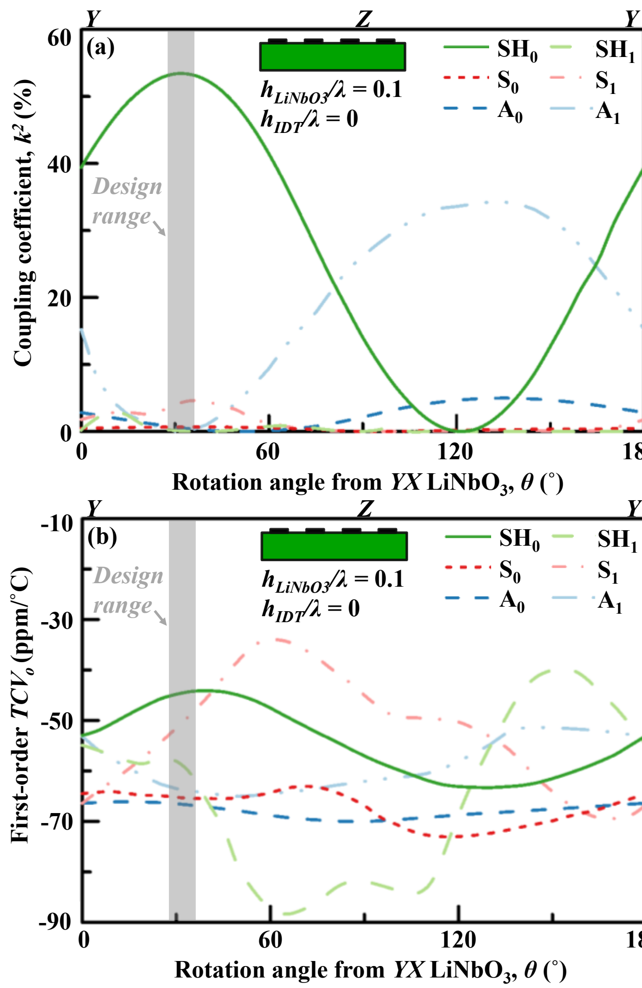

Fig. 1. Calculated (a) phase velocity and (b) first-order *TCV* versus rotation angle of the first six Plate modes in the rotated *YX* $LiNbO_3$ membrane (h_{LiNbO3}/λ=0.1) when the mechanical loading of IDT is ignored (h_{IDT}=0).

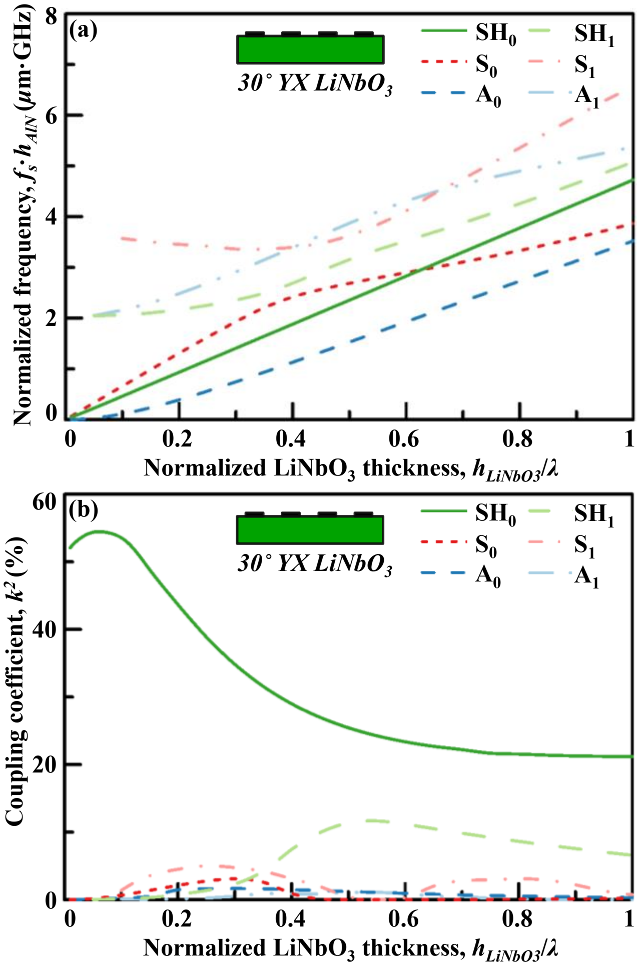

Fig. 2. Calculated (a) *f*-*β* dispersion curve and (b) dispersive k^2 of the first six Plate modes in the 30° *YX* $LiNbO_3$ membrane ($h_{IDT} = 0$).

II. SH$_0$ Plate Wave Propagating in LiNbO$_3$ Membrane

A. Cut Angle

Fig. 1 (a) and (b) show the k^2 and temperature coefficient of velocity (*TCV*) across all rotation angle from the *YX* $LiNbO_3$ for the first six Plate modes with $h_{LiNbO3}/\lambda = 0.1$ (λ is twice the IDT pitch). The k^2 varies largely due to the prominent anisotropy of the piezoelectric matrix, so the optimal cut angle can be chosen so as to optimize the k^2. The peak k^2 of 55% happens at rotation angle of ~30° with Euler angle (0°,120°,0°). It is also interesting to note that at this rotation angle of around 30°, the k^2's of most other Plate modes are minimized, especially the A_1 Lamb mode that is outstanding around *Z*-cut.

The *TCV* can be derived from the temperature coefficients of elasticities (*TCE*'s) and temperature dependence of density of $LiNbO_3$ [7]. By adding the effect of *TCV* together with the thermal expansion coefficient (α), *TCF* can be estimated as:

$$TCF_{1st} = \frac{1}{f}\frac{\partial f}{T} = \frac{1}{v}\frac{\partial v}{T} - \alpha_x = TCV_{1st} - \alpha_x \tag{1}$$

The α_x of $LiNbO_3$ is around 15.4 ppm/°C so that the $LiNbO_3$ plate based resonators show very poor intrinsic *TCF* of -60—100 ppm/°C. Luckily at the rotation angle of ~ 30° the *TCV* of the SH_0 mode is minimized across the entire cut angle.

B. Dispersion

The dispersion characteristics of the first six Plate waves propagating in the 30° *YX* $LiNbO_3$ with h_{LiNbO3}/λ =0.1 are shown in Fig. 2 (a). The normalized wave number of the *x* axis corresponds to normalized $LiNbO_3$ plate thickness:

$$\frac{\beta \cdot h_{LiNbO3}}{2\pi} = \frac{h_{LiNbO3}}{\lambda}. \tag{2}$$

Evidently, the SH_0 mode shows weakest dispersion and features the advantage of pitch-controlled frequency even when the $LiNbO_3$ plate thickness approaches zero. In addition, the low dispersion of the fundamental modes also allows the agile design of the acoustic-coupled filters [6].

Fig. 2 (b) depicts the dispersive k^2 of the first six Plate waves for the single-IDT transducer configuration in the 30° *YX* $LiNbO_3$. At this cut angle of (0°,120°,0°), the SH_0 mode features very large k^2 while the other modes are suppressed. Especially when $LiNbO_3$ is thin (< 0.2λ), the k^2 is higher than 40% and clean wide-band spectrum is expected.

III. SH$_0$ Wave Characteristics in LiNbO$_3$/SiO$_2$ and SiO$_2$/LiNbO$_3$/SiO$_2$

A. Phase Velocity Degradation

The piezoelectric-dead SiO_2 layer loads the $LiNbO_3$ thin film and significantly reduces the phase velocity (v_p) of the SH_0 mode in the $LiNbO_3/SiO_2$ membrane, as shown in Fig. 3. The v_p of the SH_0 mode in the symmetrical $SiO_2/LiNbO_3/SiO_2$ membrane is higher than that in the $LiNbO_3/SiO_2$ bilayer structure, especially when the thicker SiO_2 layer is utilized and h_{LiNbO3}/λ is small. At thin $LiNbO_3$ with h_{LiNbO3}/λ =0.1 the SH_0 mode in the SiO_2/ $LiNbO_3/SiO_2$ membrane shows the phase velocity of roughly 4,280 m/s and in the $LiNbO_3/SiO_2$ bilayer structure around 4,200 m/s at $h_{SiO2}/\lambda = 0.2$.

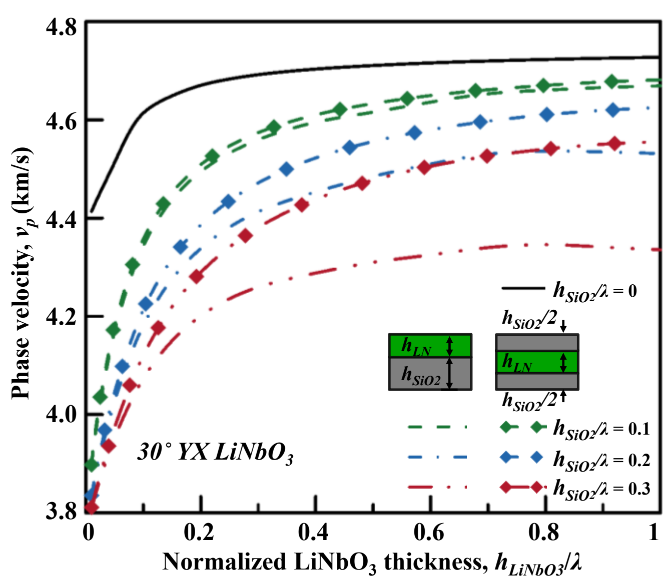

Fig. 3. Comparison of the FEA simulated v_p dispersion of the SH_0 mode in the $LiNbO_3/SiO_2$ bilayer membrane and in the symmetrical $SiO_2/LiNbO_3/SiO_2$ composite membrane with 30° *YX* $LiNbO_3$.

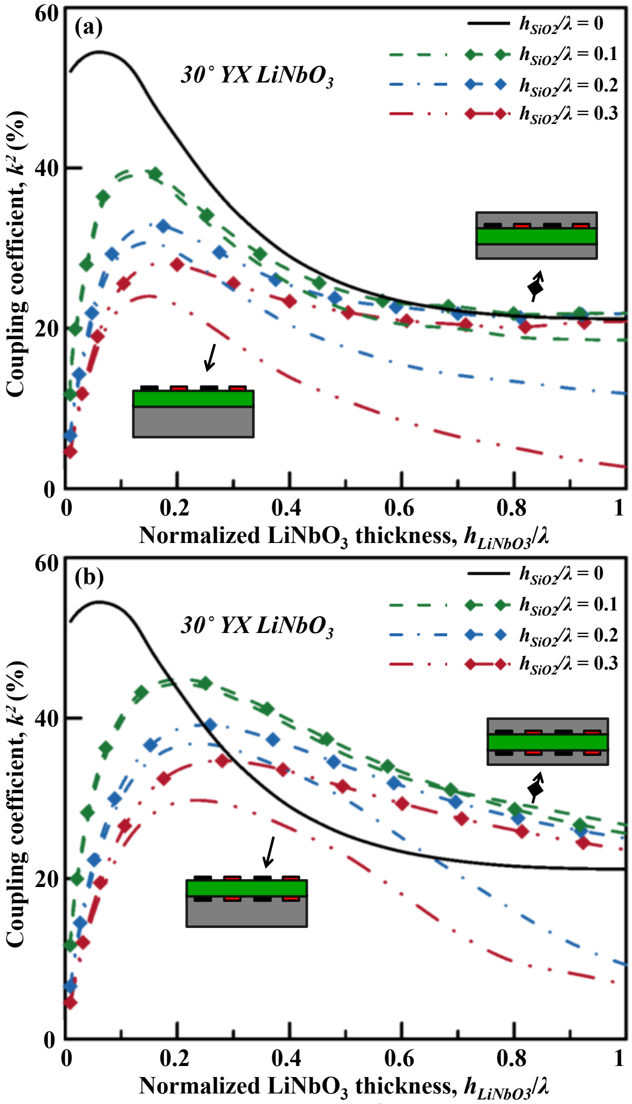

Fig. 4. Comparison of the FEA simulated k^2 dispersion utilizing the SH_0 mode in the $LiNbO_3/SiO_2$ bilayer membrane and in the symmetrical SiO_2/ $LiNbO_3/SiO_2$ composite membrane with (a) single-IDT and (b) double-IDT.

B. Coupling Coefficient Degradation

As depicted in Fig. 4, the k^2 dispersion curves of the SH_0 mode on the $LiNbO_3/SiO_2$ and $SiO_2/LiNbO_3/SiO_2$ composite membrane are compared with single-IDT and double-IDT transducer configurations. The k^2 is usually deteriorated by the additional SiO_2 layer because of the acoustic energy absorption by the piezo-dead and soft SiO_2 layer. Since the acoustic wave field tends to be more involved in the $LiNbO_3$ layer of the symmetrical $SiO_2/LiNbO_3/SiO_2$ plate, the acoustic energy can be confined in the $LiNbO_3$ plate to enable a higher k^2 for the SH_0 mode. As a result, especially when thick SiO_2 layers are employed, the k^2 of the SH_0 mode in the $SiO_2/LiNbO_3/SiO_2$ sandwiched plate is larger than in the $LiNbO_3/SiO_2$.

Intriguingly, for some cases the k^2 of the SH_0 mode in the layered plates can be even larger than that in the $LiNbO_3$ single plate. For example when h_{LiNbO3}/λ = 0.3–1 is employed for double-IDT and double-SiO_2, the k^2 is much increased, where the growing contribution of the e_{15} piezoelectric constant by the surface constraint overcomes the loading effect.

C. TCF and Trade-Off

Neglecting the electrode thickness, the first-order *TCF*'s of the $LiNbO_3/SiO_2$ and $SiO_2/LiNbO_3/SiO_2$ SH_0 resonators can be theoretically predicted and are depicted in dashed lines of Fig. 5 and Fig. 6. By adding the SiO_2 layers onto the $LiNbO_3$ thin film, the *TCF*'s increase fast and cross 0 ppm/C°. However, the first-order *TCF*'s in the $SiO_2/LiNbO_3/SiO_2$ plate are slightly smaller than in the $LiNbO_3/SiO_2$ plate at the same h_{LiNbO3}/λ and h_{SiO2}/λ, giving opposite preference for selecting stack configuration from considering v_p and k^2. In addition, there is also a general trade-off relation between the *TCF* and k^2 for selecting the stack thicknesses.

In order to compare the trade-offs, the k^2 values at zero *TCF* are identified and marked in dots in Fig. 5 and Fig.6. In general, the SH_0 mode in the sandwiched structure still offers a slightly larger k^2 than in the bilayer plate, especially at greater $LiNbO_3$ thicknesses. The simplest zero-*TCF* stack can be $LiNbO_3/SiO_2$ with $h_{LiNbO3}/\lambda = 0.1$, $h_{SiO2}/\lambda = 0.2$, and single-IDT. It is also interesting to notice that for double-IDT and double-SiO_2 the k^2 can be large (~30%) even at a thicker $LiNbO_3$ at zero-*TCF*, showing potential for the multi-frequency application (large pitch variation in the same stack).

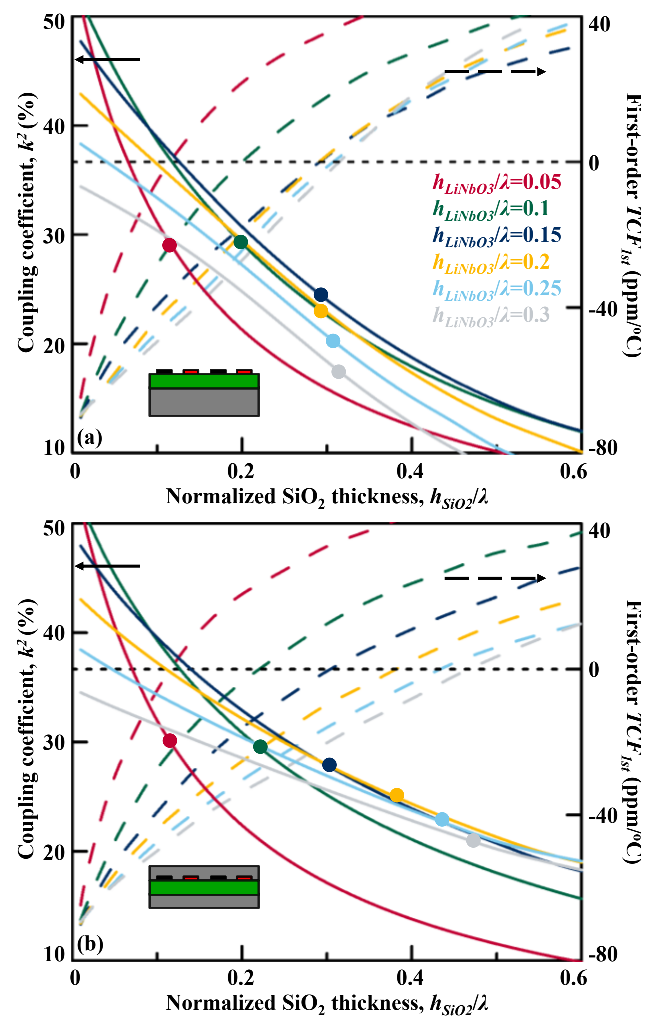

Fig. 5 Trade-off between the first-order TCF_{1st} and intrinsic k^2 of the SH_0 mode in the $LiNbO_3/SiO_2$ bi-layer structure and symmetrical $SiO_2/LiNbO_3/SiO_2$ composite membrane with single-IDT transducer.

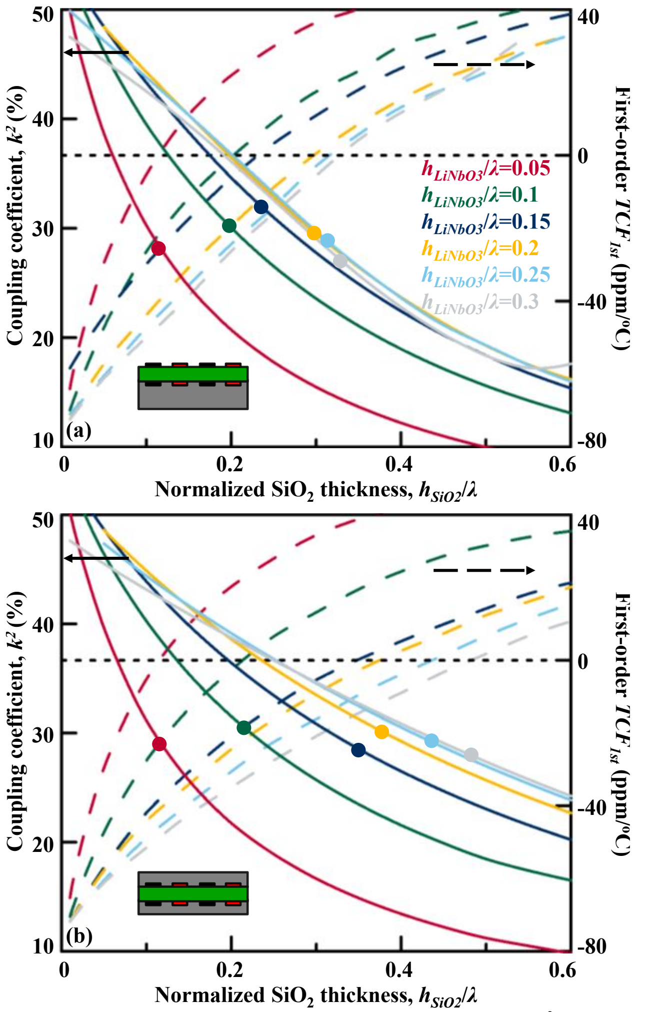

Fig. 6. Trade-off between the first-order *TCF* and intrinsic k^2 of the SH_0 mode in the $LiNbO_3/SiO_2$ bi-layer structure and symmetrical $SiO_2/LiNbO_3/SiO_2$ composite membrane with double-IDT transducer.

IV. Dispersion

The periodically perturbed dispersion of the SH_0 wave propagating in $LiNbO_3$ membrane determined by the presence of a frequency stopband [8] will be impacted by adding the SiO_2 layer. The open-circuited (OC) dispersion analysis of the SH_0 wave travelling in the $LiNbO_3/SiO_2$ bilayer structure with near-zero *TCF* (h_{LiNbO3}/λ = 0.1 and h_{SiO2}/λ = 0.2) is provided in Fig. 7. For the OC boundary condition, the non-excited modes appear in the lower stopband edge when IDT is relatively thin (h_{IDT}/λ = 4% and h_{IDT}/λ = 6%) and start to be at the upper stopband edge when the IDTs become thicker (h_{IDT}/λ > 6%).The phenomenon of the non-excited mode below the OC excitable mode (f_p) is rare and detrimental to the passband performance. In this case, the short-circuited (SC) reflection coefficient is not enough to cover the OC excitable mode, and the OC reflection coefficient is negative. As a result, it is critical to use thicker IDT electrodes for the SH_0 resonators.

V. Conclusions

The thermal stabilization techniques for the SH_0 mode in $LiNbO_3$ PAW resonators is investigated using the $LiNbO_3/SiO_2$ and $SiO_2/LiNbO_3/SiO_2$ structures. The $SiO_2/LiNbO_3/SiO_2$

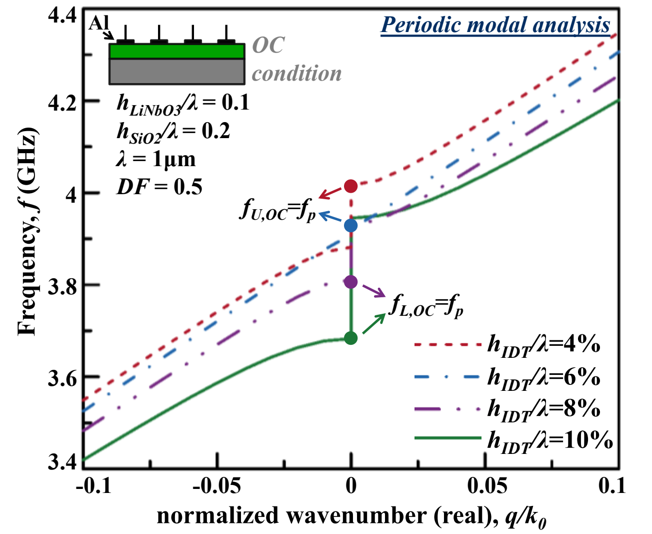

Fig. 7. Real part of the SH_0 propagation constant in single-IDT and open-circuited condition for different electrode thicknesses of the SH_0 mode propagating in the $LiNbO_3/SiO_2$ bilayer structure assuming λ = 1μm, h_{LiNbO3}/λ = 0.1, h_{SiO2}/λ = 0.2 and *DF* = 0.5.

sandwiched membrane enables higher v_p and larger k^2 than the $LiNbO_3/SiO_2$ bilayer since the symmetric structure traps more acoustic field in the $LiNbO_3$ piezoelectric layer. By considering the trade-off between *TCF* and k^2, simplest zero-*TCF* stack is proposed as $LiNbO_3/SiO_2$ with h_{LiNbO3}/λ = 0.1, h_{SiO2}/λ = 0.2, and single-IDT. The dispersive stopband analysis is given for this structure and the threshold IDT thickness of 8% is provided for wide enough stopband *BW* covering passband. Intriguingly, the $SiO_2/LiNbO_3/SiO_2$ structure with double-IDTs offers a wide selection of thickness combinations for simultaneously enabling large k^2 and zero-*TCF*, showing potential for the multi-frequency applications.

References

[1] M. Kadota, Y. Kuratani, T. Kimura, M. Esashi1, and S. Tanaka, "Ultra-wideband and high frequency resonators using shear horizontal type plate wave in LiNbO3 thin plate," *Jpn. J. Appl. Phys.*, vol. 53, 07KD03, June 2014.

[2] M. Kadota and S. Tanaka, "Ultra-wideband ladder filter using SH0 plate wave in Thin $LiNbO_3$ plate and its application to tunable filter," *IEEE Trans Ultrason Ferroelectr Freq Control*, vol. 62, May. 2015.

[3] J. Zou, F. Iliev, R. B. Hammond, V. Plessky, S. Samadian, P. J. Turner, V. Yantchev, and N. O. Fenzi, "Design of Ultra-Large-Coupling SH_0 Plate Wave Resonators on $LiNbO_3$ with Clean Spectrum," *in IEEE Intl. Freq. Control Symp. (IFCS'19),* Orlando, FL, USA, May 2019.

[4] V. Plessky, S. Yandrapalli, P.J. Turner, L.G. Villanueva, J. Koskela and R.B. Hammond, "5 GHz laterally-excited bulk-wave resonators (XBARs) based on thin platelets of lithium niobate," *Electronics Letters*, vol. 55, Nov. 2018.

[5] M.-H. Li, R. Lu, Y. Yang, T. Wu, and S. Gong, "Temperature Stability Analysis of Thin-Film Lithium Niobate SH0 Plate Wave Resonators," *J. Microelectromech. Syst.*, early access.

[6] J. Zou, C.-M. Lin, A. Gao, and A. P. Pisano, "The multi-mode resonance in AlN Lamb wave resonators," *J. Microelectromech. Syst.*, vol. 27, issue 6, pp. 973-984, Dec. 2018.

[7] R. T. Smith and F. S. Welsh, "Temperature dependence of the elastic, piezoelectric and dielectric constants of Lithium Tantalate and Lithium Niobate," *J. Appl. Phys.*, vol. 42, pp. 2219–2230, May 1971.

[8] V. Yantchev, "Coupling-of-Modes Analysis of Thin Film Plate Acoustic Wave Resonators Utilizing the S0 Lamb Mode," *Trans Ultrason Ferroelectr Freq Control*, vol. 57, Apr. 2010.